Density Functional Studies of the Reactions of Lanthanide Monocations with Fluoromethane: C−F Bond Activation and Electron-Transfer Reactivity

Dongju Zhang, Chengbu Liu,* and Siwei Bi

Institute of Theoretical Chemistry, Shandong University, Jinan, 250100, People's Republic of China

Received: October 9, 2001; In Final Form: February 5, 2002

The reactivity of lanthanide monocations with fluorinated hydrocarbons has been investigated for the first time by using density functional theory. The potential energy surfaces of [Ln, C, H_3, F]$^+$ (Ln = Ce, Pr, and Yb) were explored in detail. A direct abstraction mechanism of fluorine atom by Ln^+ was revealed, and the related thermochemistry data were determined. The electron-transfer reactivities of the reactions were analyzed by the two-state model, and a strongly avoided crossing behavior on the transition state regions for all the three systems was shown. The present results support the reaction mechanism inferred from early experimental data, and the related thermochemistry data given here can provide a guide for further experimental research.

Introduction

It is well-known that the C−F bond in organic compounds is significantly stronger than the corresponding C−H and C−C bonds and that C−F bond activation is a formidable task in organometallic chemistry.[1] In recent years, C−F bond activation by metal centers has attracted a great deal of interest,[2−6] and many theoretical and experimental studies have shown that bare metal monocations are able to activate the C−F bond selectively.[5−9] Ridge and co-workers[7] reported the first case of C−F bond activation by Fe^+ in its reaction with fluorobenzene in the gas phase. Recently, Schwarz and co-workers[6] demonstrated the gas-phase reactions of several bare lanthanide monocations Ln^+ (Ln = Ce, Pr, Sm, Ho, Tm, Yb) with various fluorinated hydrocarbons. The main reaction pathway proposed in all cases was C−F bond activation to form LnF^+ and the corresponding neutral radicals of various hydrocarbons. They proposed a "harpoonlike" mechanism with a [Ln---FCH_3]$^+$-type intermediate and a [Ln^{2+}---F^----CH_3]-type transition state.

As a supplement to the experimental studies reported by Schwarz and co-workers, we present here further theoretical study of the reactivity of lanthanide monocations with fluorinated hydrocarbons. The systems selected here are $Ln^+ + CH_3F$ (Ln = Ce, Pr, and Yb). Where three lanthanide cations are selected as representatives of the 4f row, Ce is one of the most reactive lanthanides, Pr is a more reactive element of 4f row, and Yb was found to be the element of the general "onset" in reactivity of the hole series.[6] The main aim in the present study is to give a qualitative model that explains how the lanthanide monocations Ln^+ activate the C−F bond in fluorohydrocarbons. In addition, we also calculated related thermochemistry data of the reaction, which can act as a guide for future experimental research. Our focus in this work is to learn more details about the reaction mechanism for the $Ln^+ + CH_3F$ cationic systems and to analyze the electron-transfer reactivities of the reactions. The theoretical predictions presented here for the reactions of selected Ln^+ with CH_3F can provide a template for further comprehension of the reactions of lanthanide monocations with fluorohydrocarbons.

* Corresponding author: Tel +86-531-8378718; fax +86-531-8364464; e-mail cbliu@sdu.edu.cn.

It is well-known that theoretical research for systems involving lanthanide is very difficult to deal with in ab initio Hartree−Fock theory since a relatively large number of electrons is present in these systems. As an alternative, density functional theory (DFT)[10,11] has recently attracted considerable attention and has been widely applied to electronic structure calculations for systems containing transition metals. The electron correlation effect in these systems is expected to play an important role in determining the system energetics as well as the electronic configurations. The DFT method has been shown to be particularly useful and computationally efficient for systems with a relatively large number of electrons that are difficult to deal with in ab initio Hartree−Fock theory.[12,13] In the present study, structure optimizations and energetics evaluations for the intermediates and first-order saddle point on the PESs [Ln, C, H_3, F]$^+$ (Ln = Ce, Pr, and Yb) are carried out by the gradient-corrected DFT method under the generalized gradient approximation (GGA).[14]

Computational Method

The present calculations employ all electrons in the system, and the DFT method used in our calculations is provided by the Dmol3 programs.[15] We first optimized the structures of all the stationary points (reactants, products, intermediates, and transition states) on the PESs [Ln, C, H_3, F]$^+$ (Ln = Ce, Pr, and Yb) at the GGA level. Then the vibrational frequencies are obtained at the same theoretical level to determine the nature of these stationary points and the zero-point vibrational energy (ZPE). The stationary points on the PES have been identified for minima (number of imaginary frequencies NIMG = 0) or the first-order saddle points (NIMG = 1) from the analytically computed force-constant matrix. To ensure good accuracy, the Kohn−Sham equation is solved by using a double numerical basis set augmented with polarization functions and employing the "finegrid" option for the atomic integration grids. Since the relativistic effects are expected to be significant for heavy elements, so in the present calculation this effect has been taken into account for all electrons, which is more accurate than an effective core potential calculation. The PW91[16] exchange and correlation functionals are used in the GGA calculations. The

10.1021/jp015557v CCC: $22.00
Published on Web 03/23/2002

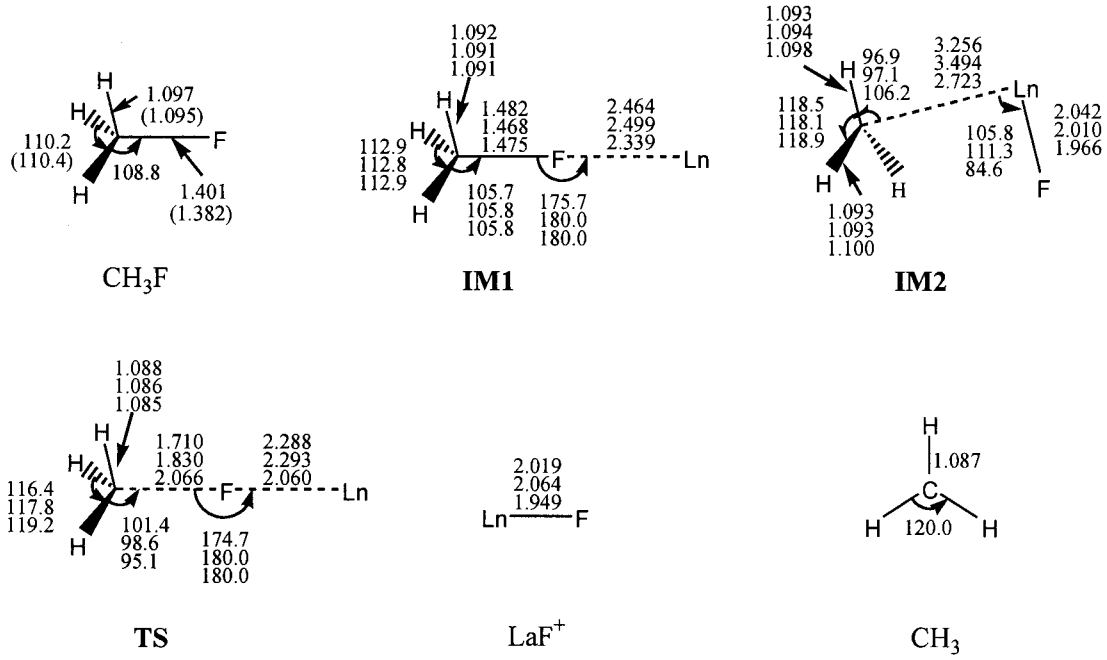

Figure 1. Optimized structures for the stationary points on the potential energy surface of [Ln, C, H_3, F]$^+$ (Ln = Ce, Pr, and Yb). The geometrical parameters are arranged in the order Ce, Pr, and Yb from the top down. The values in italic type are experimental results. Distances are in angstroms and angles are in degrees.

spin-polarized computational scheme was utilized throughout this work to deal with the electronically open-shell systems.

Results and Discussion

Calibration. To check whether DFT can be used successfully for the selected fluorine-containing systems and to estimate the level of accuracy that can be expected from our computational strategy, we commence our study with a comparison of experimentally known data to the relevant species of $Ln^+ + CH_3F$ systems.

For CH_3F, the optimized geometry parameters are shown in Figure 1, where the C−F bond length is 1.400 (1.382) Å and relevant vibration frequencies are 1018 (1049), 1149 (1182), 1149 (1182), 1434 (1464), 1454 (1464), 1454 (1467), 3033 (2938), 3121 (3006), 3126 (3006) cm^{-1}, respectively. Furthermore, the bond energy of CH_3−F is 115.33 (112 ± 0.3) kcal/mol. The values in parentheses are the experimental results. It is found that our calculated results are in good agreement with the experimental findings. For the LaF^+ diatom species and the complexes of Ln^+ with CH_3F, however, neither geometries nor the precise experimental values of thermochemistry data are available. Kaledin et al.,[17] however, estimated the bond dissociation energies for all LnX^+ (where X = F, Cl, Br, or I) by combining thermochemical data for the lanthanide monohalides with ligand theory calculations.[18] It was found in their work that the values of bond dissociation energies are 146.38, 146.09, and 133.23 ± 3.43 kcal/mol for Ce^+−F, Pr^+−F, and Yb^+−F species, respectively. Recently, Schwarz and co-workers[6] also estimated the bond dissociation energies of Ln^+−F diatomic species from the experimental data, where a lower bound of 123 kcal/mol was proposed. The theoretical values of the bond energies of Ln^+−F species obtained in the present work are 151.20, 138.34, and 123.63 ± 0.3 kcal/mol for Ce^+−F, Pr^+−F, and Yb^+−F species, respectively. These values are comparable with the experimental values estimated from the relevant thermochemistry data.

The above results lead us to conclude that the theoretical level used in this work is capable of describing the basic electronic characteristics of the species of interest.

TABLE 1: Relative Energies of the Species Involved in Reaction of $Ln^+ + CH_3F$ (Ln = Ce, Pr, and Yb)[a]

	$Ce^+ + CH_3F$	$Pr^+ + CH_3F$	$Yb^+ + CH_3F$
$Ln^+ + CH_3F$	0.00	0.00	0.00
IM1	−27.19	−22.84	−19.86
TS	−21.00	−12.28	−10.84
IM2	−56.22	−36.11	−29.63
$LnF^+ + CH_3$	−38.20	−26.34	−11.55

[a] Energies are given in kilocalories per mole.

Geometries and Energies. For the [Ln, C, H_3, F]$^+$ (Ln = Ce, Pr, and Yb) systems, very similar structures of the intermediates and transition states are found in the corresponding PESs. The optimized geometry parameters are shown in Figure 1, and relevant energies are collected in Table 1.

IM1s are reactant-like intermediates, which are initially formed as Ln^+ and CH_3F approach each other. The electronic ground states of these initially formed ion/molecule complexes are found to be quartet, quintet, and doublet for the systems of Ce^+, Pr^+, and Yb^+ with CH_3F, respectively. The relative energies are computed to be 27.19, 22.84, and 19.86 kcal/mol more stable, respectively, than the corresponding $Ln^+ + CH_3F$ entrance channels. Both the C−F bond lengths and H−C−H angles in these complex are slightly larger compared to these in free CH_3F. Ln−F distances and Ln−F−C angles in IM1s are 2.464 Å and 175.7° for Ce^+−FCH_3, 2.499 Å and 178.8° for Pr^+−FCH_3, and 2.339 Å and 180.0° for Yb^+−FCH_3. Mulliken population analysis (MPA) shows that the charge distributions and spin densities are 0.924 and 2.999 for Ce, 0.893 and 3.991 for Pr, and 0.919 and 0.989 for Yb, respectively (see Table 2). The results indicate that the unpaired electrons are mostly located on the metal ions in IM1s and that the interactions between Ln^+ and CH_3F are electrostatic in nature, as shown by the long Ln−F bond distances and the results of the MPA. The calculated bond dissociation energies of Ln^+−FCH_3 are 27.19 kcal/mol for Ce^+−FCH_3, 22.84 kcal/mol for Pr^+−FCH_3, and 19.86 kcal/mol for Yb^+−FCH_3. This fact indicates that the electrostatic interactions between Ln^+ and CH_3F are weak. The early experimental findings[6] proposed that

TABLE 2: Mulliken Charges and Spin Densities for the IM1s and TSs Involved in the Reactions of Ln^+ with CH_3F (Ln = Ce, Pr, and Yb)

		$Ce^+ + CH_3F$			$Pr^+ + CH_3F$			$Yb^+ + CH_3F$	
		charge	spin		charge	spin		charge	spin
IM1	C	0.098	0.001	C	0.079	0.011	C	0.086	0.020
	F	−0.476	−0.004	F	−0.418	−0.005	F	−0.450	−0.009
	H	0.150	0.002	H	0.149	0.001	H	0.148	0.000
	H	0.153	0.001	H	0.149	0.001	H	0.148	0.000
	H	0.151	0.002	H	0.149	0.001	H	0.148	0.000
	Ce	0.924	2.999	Pr	0.893	3.991	Yb	0.919	0.989
TS	C	0.001	0.208	C	−0.035	0.234	C	−0.122	0.551
	F	−0.521	−0.011	F	−0.443	−0.017	F	−0.532	−0.026
	H	0.164	−0.006	H	0.164	−0.006	H	0.160	−0.019
	H	0.167	−0.006	H	0.167	−0.007	H	0.160	−0.019
	H	0.164	−0.006	H	0.167	−0.007	H	0.160	−0.019
	Ce	1.025	2.820	Pr	0.979	3.802	Yb	1.174	0.532

the initial ion/molecule complexes of lanthanide monocation with fluorohydrocarbons could be the rate-determining step of the C−F bond activation. This suggestion is in good agreement with weak electrostatic interactions between Ln^+ and CH_3F.

The structures of transition states (TSs) in Figure 1 correspond to the first-order saddle points of the C−F bond activation on the potential energy surfaces of [Ln, C, H_3, F]$^+$, which were characterized by the presence of one imaginary frequency and one negative eigenvalue in the corresponding Hessian matrixes. The ground-state energy of the TS for $Ce^+ + CH_3F$ system is 6.19 kcal/mol above the corresponding IM1 and 21.00 kcal/mol below the entrance channel, and those for $Pr^+ + CH_3F$ system are 9.56 and 12.28 kcal/mol, and those for $Yb^+ + CH_3F$ system are 9.02 and 10.84 kcal/mol. For [Ce, C, H_3, F]$^+$ system, the C−F bond in the TS is elongated by 15% and the Ce−F bond is shorted by 7%, compared to those in the corresponding IM1. For [Pr, C, H_3, F]$^+$ and [Yb, C, H_3, F]$^+$ systems, C−F bonds are elongated 15% and 40%, and Ln−F bonds are shorted by 8.4% and 12%, respectively. Obviously, the transition states are tightly bonded structures. In all three TSs, the Ln−F−C angles are almost unchanged compared to the structures of IM1s. The corresponding transition vectors indicated by the vibration analysis correspond to the breaking of the C−F bond and the forming of the Ln−F bond. In Table 2, the charge distributions and spin densities for each TS are compared with those of the corresponding IM1. It is very clear that the electron transfer has occurred from Ln^+ to CH_3F, as indicated by the tight transition-state structures and MPA. The electron transfer from the 6s orbital of Ln^+ to the σ^* orbital of CH_3F favors the homolytic cleavage of the C−F bond to form the LnF^+ species and CH_3 radical.

The other minima on the PESs are formally the insertion products of Ln^+ into the C−F bond, denoted as IM2s, and their energies are calculated to be 56.22 kcal/mol more stable than the respective entrance channels for the $Ce^+ + CH_3F$ system, 36.11 kcal/mol for the $Pr^+ + CH_3F$ system, and 29.63 kcal/mol for the $Yb^+ + CH_3F$ system. These formal insertion products, in which the C−F bond has already ruptured and $Ln^{+-}F$ bonds have formed, are global minima on the PESs of [Ln, C, H_3, F]$^+$. The Ln−F lengths and the geometry parameters of CH_3 units in these complexes have resembled those of the free Ln−F species and CH_3 free radical. Obviously, its exit channel is to form LnF^+ diatomic species and CH_3 free radical.

Reaction Mechanism. Now let us analyze the mechanism of the reactions of Ln^+ with fluoromethane. Recently, it was observed that Ln^+ can selectively activate the C−F bond to yield LnF^+ and methyl radical in the reactions of several lanthanide cations with fluoromethane. In light of the experimental result, two alternative reaction mechanisms could be inferred for the reactions of Ln^+ with CH_3F, as shown in Scheme 1.

SCHEME 1: Experimentally Inferred Reaction Mechanism for the Reaction of Ln^+ with CH_3F

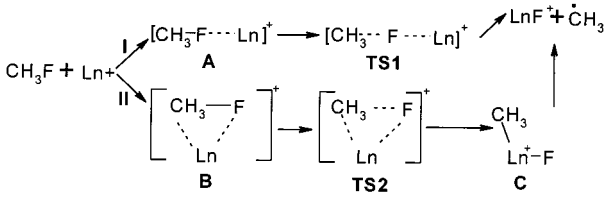

Mechanism I is a direct abstraction reaction of fluorine atom by Ln^+, where CH_3-F could first coordinate to Ln^+ through the electronegative fluorine atom to form a initial ion/molecule complex (A) of the linear type; then this complex crosses a barrier (TS1) to form the LaF^+ species and methyl radical. Mechanism II is an insertion−elimination process, in which a three-membered cyclical initial complex (B) and a three-center transition state (TS2) were postulated to insert Ln^+ into the C−F bond.

From present theoretical studies, both the reactant-like intermediates and transition state are found to be of the linear type, and the cyclic precursors B and the corresponding transition states TS2 proposed early in Scheme 1 are not found for all three systems. Despite numerous attempts to locate the cyclic precursors and transition states, no state mimima were found. However, the formal insertion intermediates IM2, as shown in Figure 1, which is denoted as C in Scheme 1, are found surely on the potential energy surfaces of [Ln, C, H_3, F]$^+$ for all the three systems. This fact suggests that the reactions of Ln^+ (Ln = Ce, Pr, and Yb) could proceed according to mechanism I, and mechanism II appears to be not available; i.e., the C−F bond activation of CH_3F is the direct abstraction reaction of fluorine atom by Ln^+. This reaction mechanism is easily understood, since all the ground states of cerium, praseodymium, and ytterbium monocations have only one non-f electron and cannot easily undergo insertion. The formal insertion intermediates of Ln^+ into the C−F bond, IM2s, however, are located along the reaction coordinate after the TSs. The intermediates are product-like complexes and are overall minima of the potential energy surfaces of [Ln, C, H_3, F]$^+$. Although we also tried to locate a product-like complex of the linear type, [Ln−F---CH_3]$^+$, no such minima were found for all three systems after careful seeking. Thus, according to present calculations, we conclude that the TSs either directly dissociate into products, $LnF^+ + CH_3$, or further convert into IM2. In terms of the clue given in this work, the reaction mechanism

SCHEME 2: Proposed Reaction Mechanism for the Reaction of Yb^+ with CH_3F from the Present Calculations

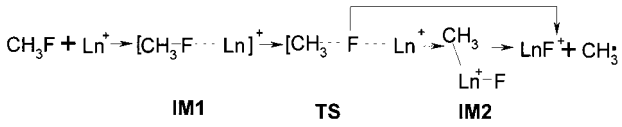

for the three systems studied here is proposed as shown in Scheme 2.

If the mechanism is similar along the 4f row elements, we conclude that the ability of Ln^+ to abstract an F atom from CH_3–F should be related to the second ionization energy of the lanthanide monocations. Schwarz and co-workers observed the different reactivities of six lanthanides with CH_3F and found that the lower the second ionization energy of the lanthanide, the higher its abstraction reactivity on the fluorine atom in CH_3F. Hence, they also proposed that these reactions are direct abstraction reactions of F atom by Ln^+. This conclusion is in line with our suggestion.

The reaction mechanism proposed for the selected three systems is very similar to that given by Schwarz for the reaction of Ca^+ with CH_3F.[8]

The potential energy surface profiles of the reactions of Ln^+ with CH_3F are shown in Figure 2.

Heat of Reaction and Bond Dissociation Energy. As far as we know, no precise thermochemical information is available for the reactions $Ln^+ + CH_3F \rightarrow LnF^+ + CH_3$. In the present work, the calculated heats of reaction are exothermic by 38.20 kcal/mol for the $Ce^+ + CH_3F$ system, by 26.34 kcal/mol for the $Pr^+ + CH_3F$ system, and by 11.63 kcal/mol for the $Yb^+ + CH_3F$ system. If the theoretical values are used, together with a value of 112 ± 0.3 kcal/mol for the bond dissociation energy (BDE) of the C−F bond in fluoromethane, the BDE of diatomic species Ln^+−F are determined to be 151.20 kcal/mol for Ce^+−F, 138.34 kcal/mol for Pr^+−F, and 123.63 ± 0.3 kcal/mol for Yb^+−F. These values are comparable with those estimated by Kaledin et al.[17] and also with a lower bound of 123 kcal/mol, proposed by Schwarz and co-workers.[6]

Potential Energy Surface Crossing Behavior on the Transition-State Area. To study the electron-transfer reactivity in the reactions of Ln^+ with CH_3F, we now analyze the potential energy surface crossing behaviors on the transition-state areas by using a two-state model of the electronic structure. Since both the wave functions of IM1 and IM2, which correspond respectively to a reactant-like species and a product-like species and clearly differ by a single electron transfer from the 6s orbital of Ln^+ to the σ^* orbital of CH_3F, they should in principle mix and avoid the crossing. IM1 is an electrostatic complex between Ln^+ and CH_3F and a 6s electron is basically located on the metal ion. Along the reaction coordinate, the electron transfer occurs from Ln to F, which favors the homolytic cleavage of the C−F bond to form IM2. Consequently, IM1 correlates with an excited state of IM2 and the corresponding excited energy approximately equals the difference between the second ionization energy (IE) of lanthanide and the electron affinity (EA) of CH_3F. Similarly, IM2 correlates with the excited state of IM1, and the excited energy can be approximated by the difference between the ionization energy of the CH_3 radical and the electron affinity of the LnF^+ species. In present calculations, vertical excited energies of the reactant-like and product-like species are 325.50 and 103.45 kcal/mol for the $Ce^+ + CH_3F$ system, 372.03 and 113.5 kcal/mol for the $Pr^+ + CH_3F$ system, and 375.35 and 87.66 kcal/mol for the $Yb^+ + CH_3F$ system, respectively.

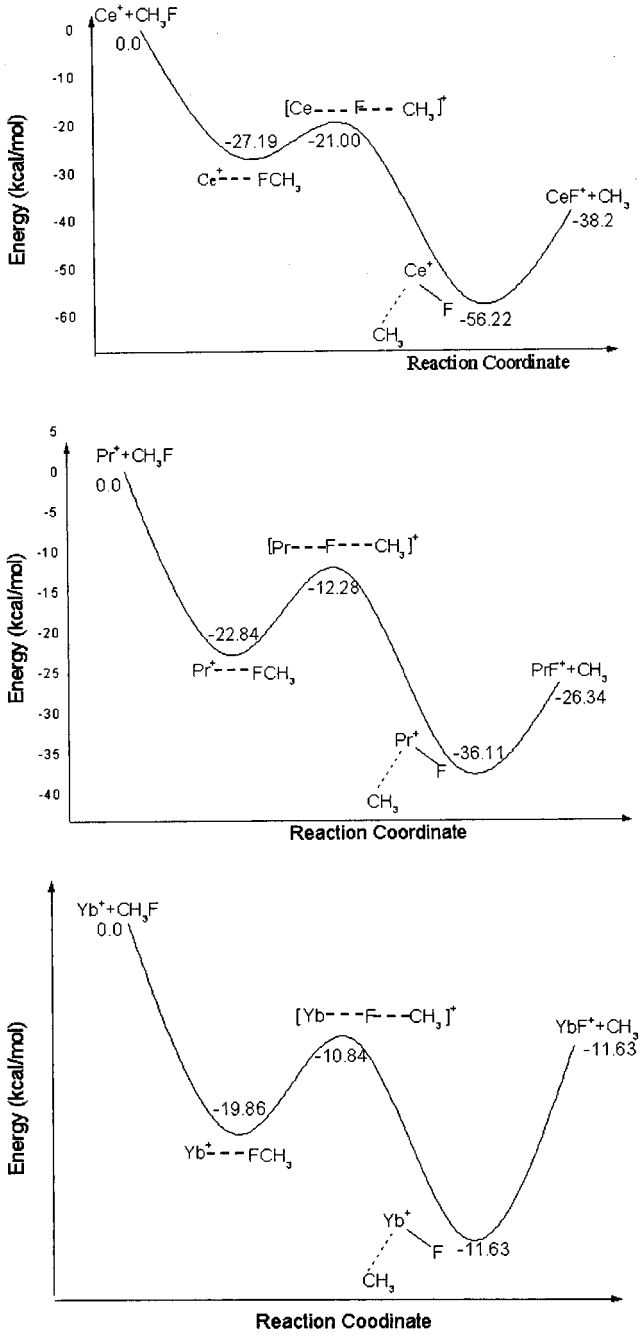

Figure 2. Potential energy surface profile of the reaction of Ln^+ with CH_3F.

To study the electron-transfer reactivity of the crossing regions on the potential energy surfaces of $[Ln, C, H_3, F]^+$, we denote the electronic state energies of the reactantlike and productlike species by E_r and E_p, respectively, when $H_{rp} = 0$. The two-state electronic secular equation at any geometry can be expressed as

$$\begin{bmatrix} E_r - E & H_{rp} - ES_{rp} \\ H_{rp} - ES_{rp} & E_p - E \end{bmatrix} = 0 \qquad (1)$$

where S_{rp} is the overlap of the two states. The difference between the two eigenvalues at the avoided crossing point, if $S_{rp} = 0$, is

$$\Delta = E_1 - E_2 = 2H_{rp} \qquad (2)$$

where H_{rp} is the matrix element coupling these two electronic

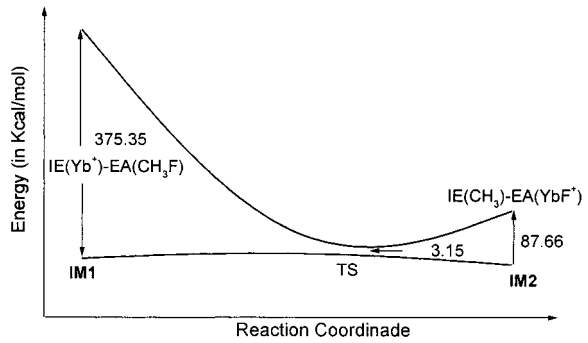

Figure 3. State correlation diagram for the reaction of Yb^+ with CH_3F.

states. The magnitude of H_{rp} determines whether the reaction proceeds adiabatically ($H_{rp} \geq RT$) or nonadiabatically ($H_{rp} \leq RT$).[19] Instead of calculating H_{rp} directly, we have calculated the state splitting at the transition state using the simple Koopmans' theorem (KT) in the Hartree−Fock method. The Hartree−Fock orbital energies correspond to the negative of IE for occupied orbitals and to the negative of the electron affinities for unoccupied orbitals. KT applies to the orbital energy difference between HOMO-1 and HOMO of the neutral system [Ln---F---CH_3], which has the geometrical parameters of the TS, and then gives the energy difference between the first excited state and the ground state. Our calculated state split energies are 10.61 kcal/mol (3710 cm^{-1}) for the $Ce^+ + CH_3F$ system, 3.57 kcal/mol (1248 cm^{-1}) for the $Pr^+ + CH_3F$ system, and 3.15 kcal/mol (1102 cm^{-1}) for the $Yb^+ + CH_3F$ system. These magnitudes of H_{rp} at the optimized transition state are larger than RT (0.59 kcal/mol, 206 cm^{-1}). The result indicates that the mixing of the two states is significant in the transition-state region for all three systems, which leads to strongly avoided crossing behavior. So it can be expected that the reactions of Ln^+ (Ln = Ce, Pr, and Yb) with CH_3F occur on an adiabatic potential energy surface and do not involve nonadiabatic surface-hopping behavior. The state correlation diagram for the $Yb^+ + CH_3F$ system is given in Figure 3. Similar results for other systems are not given for simplicity.

Conclusions

In this work we present a theoretical study of the mechanistic details and the electron-transfer reactivity for the reactions of three selected lanthanide monocations (Ln^+ = Ce, Pr, and Yb) with CH_3F, which are representative prototypes of the reactions of bare Ln^+ cations with fluorocarbons. The following conclusions can be drawn from this work.

1. The reactions of the prototype systems are a direct abstraction reaction of fluorine atom by Ln^+; i.e., after coordination of CH_3F to Ln^+, the electron transfer from Ln^+ to the fluorine takes place, and then the C−F bond homolytically ruptures to form the formally inserted species, which exits by forming LnF^+ diatomic species and methyl radical.

2. The reactions are substantially adiabatic, and the state split energies between the ground state and the first excited state were calculated to be 10.61 kcal/mol for the $Ce^+ + CH_3F$ system, 3.57 kcal/mol (1248 cm^{-1}) for the $Pr^+ + CH_3F$ system, and 3.15 kcal/mol (1101.62 cm^{-1}) for the $Yb^+ + CH_3F$ system, respectively.

3. The calculated heats of reaction for all three reactions $Ln^+ + CH_3F \rightarrow LnF^+ + CH_3$ (Ln = Ce, Pr, and Yb) are exothermic, by 38.20 kcal/mol when Ln = Ce, 26.34 kcal/mol when Ln = Pr, and 11.55 kcal/mol when Ln = Yb. The BDEs for Ln^+-FCH_3 ion/molecule complex and Ln^+−F diatomic species are 27.19 and 151.20 kcal/mol when Ln = Ce, 22.84 and 138.34 kcal/mol when Ln = Pr, and 19.86 and 123.63 kcal/mol when Ln = Yb, respectively.

Acknowledgment. We gratefully acknowledge Professor Yuansheng Jiang for many useful discussions at the School of Chemistry, Nanjing University. This work was supported by the Science Foundation of Shandong Province (under Grant Z2000B02).

Note Added after ASAP Posting. This paper was posted ASAP on 3/23/02 with an error in Ln^+−F bond energies in the Results and Discussion. The corrected paper was posted 3/27/02.

References and Notes

(1) Armentrout, P. B. *Annu. Rev. Phys. Chem.* **1990**, *41*, 313.
(2) (a) Aizenberg, M.; Milstein D. *Science* **1994**, *265*, 359. (b) Aizenberg, M.; Milstein D. *J. Am. Chem. Soc.* **1995**, *117*, 8674.
(3) Freiser, B. S. *Acc. Chem. Res.* **1994**, *27*, 353.
(4) Bjarnason, A.; Taylor, J. W. *Organometallics* **1989**, *8*, 2020.
(5) Chen, Q.; Lin, C. Y.; Chen, H.; Freiser, B. S. *Organometallics* **1997**, *16*, 4020.
(6) Cornehl, H. H.; Hornung G.; Schwarz, H. *J. Am. Chem. Soc*. **1996**, *118*, 9960.
(7) Dietz, T. G.; Chatellier, D. S.; Ridge, D. P. *J. Am. Chem. Soc.* **1978**, *100*, 4905.
(8) Harvey, J. N.; Schroder, D.; Koch, W.; Danovich, D.; Shaik, S.; Schwarz, H. *Chem. Phys. Lett.* **1997**, *278*, 391.
(9) Chen, Q.; Freiser, B. S. *J. Phys. Chem. A* **1998**, *102*, 3343.
(10) Hohenberg, P.; Kohn, W. *Phys. Rev. B* **1964**, *136*, 864.
(11) Kohn, W.; Sham, L. *Phys. Rev. A* **1965**, *140*, 1133.
(12) van Daelen, M. A.; Li. Y. S.; Newsam, J. M.; van Santen, R. A. *J. Phys. Chem*. **1996**, *100*, 2279.
(13) Ziegler, T. *Chem. Rev.* **1991**, *91*, 651.
(14) Parr, R. G.; Yang, W. *Density Functional Theory of Atoms and Molecules*; Oxford University Press: New York, 1989.
(15) $DMol^3$ (version Cerius 3.8), Molecular Simulations, Inc., 1998.
(16) Perdew, J. P. *Phys. Rev. Lett.* **1985**, *55*, 1665.
(17) Kaledin, L. A.; Heaven, M. C.; Field, R. W. *J. Mol. Spectrosc.* **1999**, *193*, 285.
(18) Kaledin, A. L.; Heaven, M. C.; Field, R. W.; Kaledin, L. A. *J. Mol. Spectrosc*. **1996**, *179*, 310.
(19) Sutin, N. *Prog. Inorg. Chem.* **1983**, *30*, 441.